



Open Access

## ORIGINAL ARTICLE

Prostate Cancer

# New model of PIRADS and adjusted prostate-specific antigen density of peripheral zone improves the detection rate of initial prostate biopsy: a diagnostic study

Chen Huang<sup>1,\*</sup>, Zong-Qiang Cai<sup>1,\*</sup>, Feng Qiu<sup>1</sup>, Jin-Xian Pu<sup>1</sup>, Qi-Lin Xi<sup>1</sup>, Xue-Dong Wei<sup>1</sup>, Xi-Ming Wang<sup>2</sup>, Xiao-Jun Zhao<sup>1</sup>, Lin-Chuan Guo<sup>3</sup>, Jian-Quan Hou<sup>1</sup>, Yu-Hua Huang<sup>1</sup>

This study explored a new model of Prostate Imaging Reporting and Data System (PIRADS) and adjusted prostate-specific antigen density of peripheral zone (aPSADPZ) for predicting the occurrence of prostate cancer (PCa) and clinically significant prostate cancer (csPCa). The demographic and clinical characteristics of 853 patients were recorded. Prostate-specific antigen (PSA), PSA density (PSAD), PSAD of peripheral zone (PSADPZ), aPSADPZ, and peripheral zone volume ratio (PZ-ratio) were calculated and subjected to receiver operating characteristic (ROC) curve analysis. The calibration and discrimination abilities of new nomograms were verified with the calibration curve and area under the ROC curve (AUC). The clinical benefits of these models were evaluated by decision curve analysis and clinical impact curves. The AUCs of PSA, PSAD, PSADPZ, aPSADPZ, and PZ-ratio were 0.669, 0.762, 0.659, 0.812, and 0.748 for PCa diagnosis, while 0.713, 0.788, 0.694, 0.828, and 0.735 for csPCa diagnosis, respectively. All nomograms displayed higher net benefit and better overall calibration than the scenarios for predicting the occurrence of PCa or csPCa. The new model significantly improved the diagnostic accuracy of PCa (0.945 vs 0.830,  $P < 0.01$ ) and csPCa (0.937 vs 0.845,  $P < 0.01$ ) compared with the base model. In addition, the number of patients with PCa and csPCa predicted by the new model was in good agreement with the actual number of patients with PCa and csPCa in high-risk threshold. This study demonstrates that aPSADPZ has a higher predictive accuracy for PCa diagnosis than the conventional indicators. Combining aPSADPZ with PIRADS can improve PCa diagnosis and avoid unnecessary biopsies.

Asian Journal of Andrology (2023) 25, 126–131; doi: 10.4103/aja202218; published online: 22 April 2022

**Keywords:** adjusted prostate-specific antigen density of peripheral zone; biopsy; diagnosis; Prostate Imaging Reporting and Data System; prostate cancer

## INTRODUCTION

Prostate cancer (PCa) is a common male cancer that affects approximately 250 000 men per year worldwide.<sup>1</sup> The incidence of PCa has risen dramatically in recent years, especially in China, where it ranks second among male tumors.<sup>2</sup> Prostate biopsy is considered the gold standard for the diagnosis of PCa.<sup>3</sup> The 12-core systematic prostate biopsy is widely used worldwide,<sup>4</sup> and is based on random sampling. However, it cannot accurately target the region of interest.<sup>5</sup> This limitation can result in false-negative results, misdiagnosis of high-risk PCa, or even overdiagnosis. According to previous reports, more than 20% of patients who have undergone an initial prostate biopsy show false-negative results, and are therefore misdiagnosed.<sup>6</sup> Multiparameter magnetic resonance imaging (mpMRI) has been increasingly used to diagnose patients with PCa.<sup>7,8</sup> In 2012, the European Society of Urogenital Radiology (ESUR) established a series of guidelines for the interpretation of mpMRI images using a

structured reporting scheme called Prostate Imaging Reporting and Data System (PIRADS).<sup>9</sup> In 2015, the American College of Radiologists, EUSR and the AdMeTech Foundation improved and updated PIRADS to version 2 (PIRADS V2).<sup>10</sup> This guideline has an important clinical significance in PCa diagnosis.<sup>11</sup> Recently, some studies have shown that prostate-specific antigen density (PSAD), PSAD of the peripheral zone (PSADPZ), and peripheral zone volume ratio (PZ-ratio) can be used to predict the occurrence of PCa.<sup>12–14</sup> In this paper, we established a new model to increase the detection rates of PCa and clinically significant PCa (csPCa), and compared its diagnostic performance with the conventional model (age, prostate-specific antigen [PSA], free/total PSA [f/tPSA], and PSAD).

## PATIENTS AND METHODS

### Ethical approval

All patients were counseled about the risks of the procedure, and then, they signed consent form that included permission to use their clinical

<sup>1</sup>Department of Urology, The First Affiliated Hospital of Soochow University, Suzhou 215006, China; <sup>2</sup>Department of Radiology, The First Affiliated Hospital of Soochow University, Suzhou 215006, China; <sup>3</sup>Department of Pathology, The First Affiliated Hospital of Soochow University, Suzhou 215006, China.

\*These authors contributed equally to this work.

Correspondence: Dr. YH Huang (sdfyymnwkyh@163.com)

Received: 14 November 2021; Accepted: 11 March 2022

data for research. Ethical approval was obtained from the Institutional Review Board of The First Affiliated Hospital of Soochow University (Suzhou, China; No. 2021237)

### Patient recruitment

In this retrospective cohort study, patients with PCa were recruited at The First Affiliated Hospital of Soochow University from June 2016 to August 2020. A total of 853 male patients who presented to our institution for prostate biopsy, accompanied by an abnormal digital rectal examination (DRE) and/or an elevated PSA level, were offered prebiopsy mpMRI. Of these patients, 48 (5.6%) had prior treatment, 67 (7.9%) had PSA >100 ng ml<sup>-1</sup>, 23 (2.7%) were not able to undergo MRI examination, and the remaining 715 (83.8%) received a transperineal prostate biopsy.

### MRI acquisition

All patients were subjected to 3T magnetic resonance (MR) scanner (MAGNETOM Skyra; Siemens Healthineers, Erlangen, Germany). The 18-channel body and standard spine array coils were employed for signal reception. The transverse T1-weighted turbo spin-echo (TSE) images, as well as the transverse, coronal, and sagittal T2-weighted TSE images of the prostate and seminal vesicles were acquired. The apparent diffusion coefficient was obtained from diffusion-weighted imaging (DWI), and was calculated using a two-dimensional (2D) echo-planar imaging sequence with multiple b-value acquisitions (0 s mm<sup>-2</sup>, 100 s mm<sup>-2</sup>, 800 s mm<sup>-2</sup>, 1000 s mm<sup>-2</sup>, and 1500 s mm<sup>-2</sup>), with diffusion-sensitizing gradients applied along the x-, y-, and z-axes. Dynamic contrast-enhanced (DCE) imaging was conducted through a three-dimensional (3D) T1-weighted gradient-echo volumetric interpolated breath-hold examination, and was in the same plane as the 3D T2W sequence. Then, an intravenous contrast agent (Medtron AG, Saarbruecken, Germany) was administered at 1 ml kg<sup>-1</sup> body weight and 2.5 ml s<sup>-1</sup> injection rate. The MR Tissue4D software (Syngo. via VA20B; Siemens Healthineers) was used to construct perfusion curves.

### Prostate biopsy and pathology analysis

Transperineal prostate-targeted biopsy (TB) and systematic biopsy (SB) were performed on all patients. During TB, the DICOM data of mpMRI images, including T2-weighted imaging (T2WI), DWI, apparent diffusion coefficient (ADC), and DCE, were imported into the Real-time Virtual Sonogra (RVS) ultrasonography host (Preirus, Hitachi, Japan), and the target lesion was marked as region of interest (ROI). Through RVS, the ROI marked on MRI images was displayed in real-time on the ultrasonography images. Ultrasonography and MRI images were matched by sagittal and axial anatomical markers, such as urethral orifices and small prostate cysts. Following these steps, the urologist performed the targeted biopsy and each ROI was executed on 2-core biopsy. After completion of TB, the RVS was turned off and the same urologist continued to perform SB. All specimens were fixed in 10% formalin and subjected to pathological analysis. The csPCa was defined as a single biopsy core with a Gleason score of 3 + 4 (7) or above (International Society of Urological Pathology [ISUP] grade group [GG] >1) as described previously.<sup>6</sup>

### Patient characteristics

The patients' age, prebiopsy PSA, f/tPSA, and pathological features were included in the study. The included MRI characteristics were PIRADS scores, prostate volume (PV) on mpMRI (PV = 0.52 × height × length × width), the PSAD (PSAD = PSA/PV), transitional zone (TZ) volume (TZV = 0.52 × height [TZ] × length [TZ] × width [TZ]), peripheral zone (PZ) volume (PZV = PV - TZV), PZ-ratio

(PZ-ratio = PZV/PV), PSADPZ (PSADPZ = PSA/PZV), and adjusted PSADPZ (aPSADPZ = PSAD × PZ-ratio). Each patient was graded according to PIRADS V2 by the same radiologist who graded more than 100 prostate MRI readings. The biopsy cores were examined by a dedicated pathologist.

### Statistical analyses

Categorical and continuous variables were analyzed using Pearson's Chi-squared test and Mann-Whitney U test, respectively. Binary logistic regression was used to calculate the odds ratios of each predictive factor. The predictive models were constructed as follows. First, univariate regression analysis was performed to evaluate the power of each parameter in diagnosing PCa and csPCa. Next, the variables with *P* < 0.05 in the univariate analysis were further analyzed by multivariate logistic regression models using the procedure of the backward selection method. The multivariate regression coefficients were then used to construct nomograms. From multivariable binary logistic analysis, the following predictive models were built to predict the occurrence of PCa and csPCa: the base model included all clinical factors such as age, PSA, f/tPSA, and PSAD, while the new model included PIRADS and aPSADPZ. The calibration and discrimination abilities of these models were evaluated using the calibration curve (1000 bootstrap resamples) and area under the receiver operating characteristic (ROC) curve (AUC), respectively. The nomograms were also validated using an internal validation cohort (1000 bootstrap resamples). The clinical benefits of these models were determined by decision curve analysis. The AUCs of both models were compared using methods described previously.<sup>15</sup> In decision curve analyses, the horizontal line along the x-axis indicated that all patients developed PCa and csPCa. The nomogram and calibration plots were constructed by R i386 4.0.2 (<http://www.r-project.org>, last accessed on March 10, 2022). Other statistical tests were conducted with SPSS version 22.0 (IBM Corp., Armonk, NY, USA) and MedCalc version 18.2.1 (MedCalc Software, Mariakerke, Belgium). All reported *P*-values were two-sided and the level of statistical significance was set at *P* < 0.05.

## RESULTS

### Demographic and clinical characteristics

Overall, 350 out of 715 patients (49.0%) had histologically confirmed PCa, while 302 (42.2%) had histologically confirmed csPCa. The clinical data of all patients are summarized in **Table 1**. PCa patients were significantly older, with higher PSA, PSAD, PZ-ratio, PSADPZ, and aPSADPZ and lower f/tPSA, PV, and TZV, compared to patients with benign disease. Similar results were observed for the differences in these parameters between csPCa group and benign or clinically insignificant prostate cancer (isPCa) group.

### Univariate and multivariate regression analyses of independent predictors for diagnosing PCa and csPCa

As shown in **Table 2**, age, PSA, f/tPSA, PV, PSAD, TZV, PZ-ratio, PSADPZ, and aPSADPZ were important predictors for diagnosing PCa and csPCa in univariate logistic regression analysis. The findings of multivariate analysis are presented in **Table 3**. Especially, age, PSA, f/tPSA, aPSADPZ, and PIRADS were included in the predictive model of PCa; while age, f/tPSA, aPSADPZ, and PIRADS were included in the predictive model of csPCa.

### ROC curve analysis of predictive factors in comparison with PSA values

ROC curve analysis revealed that the AUC for PSA in the diagnosis of PCa and csPCa were 0.669 and 0.713, respectively. Compared with

**Table 1: Patients demographics and the correlation of PIRADS with biopsy results**

Characteristic	PCa group (n=350)	Benign group (n=365)	Z	P	csPCa group (n=302)	isPCa group or benign group (n=413)	Z	P
Age (year), median (IQR)	71 (66, 76)	66 (60, 71)	-8.575	<0.01	72 (66, 76)	66 (60, 72)	-6.585	<0.01
PSA (ng ml <sup>-1</sup> ), median (IQR)	14.01 (8.20, 24.04)	8.90 (6.01, 13.86)	-7.816	<0.01	15.49 (9.38, 25.76)	8.64 (5.95, 13.82)	-3.837	<0.01
f/tPSA, median (IQR)	0.105 (0.078, 0.147)	0.151 (0.107, 0.203)	-8.263	<0.01	0.101 (0.077, 0.142)	0.150 (0.105, 0.203)	-7.020	<0.01
PV (ml), median (IQR)	35.5 (26.1, 48.6)	48.2 (33.4, 68.4)	-8.029	<0.01	35.5 (26.1, 47.9)	47.2 (32.0, 67.2)	-7.220	<0.01
PSAD (ng ml <sup>-2</sup> ), median (IQR)	0.376 (0.224, 0.701)	0.179 (0.112, 0.284)	-12.144	<0.01	0.417 (0.240, 0.798)	0.184 (0.116, 0.288)	-8.829	<0.01
TZV (ml), median (IQR)	13.8 (9.4, 21.7)	26.2 (16.2, 44.1)	-10.944	<0.01	13.5 (9.4, 20.8)	24.7 (15.3, 42.7)	-9.733	<0.01
PZV (ml), median (IQR)	20.1 (14.7, 27.4)	20.9 (15.1, 29.7)	-0.796	0.426	20.4 (14.8, 27.4)	20.7 (15.0, 29.4)	-0.990	0.322
PZ-ratio, median (IQR)	0.588 (0.506, 0.677)	0.453 (0.334, 0.549)	-11.452	<0.01	0.594 (0.510, 0.679)	0.471 (0.349, 0.561)	-9.867	<0.01
PSADPZ (ng ml <sup>-2</sup> ), median (IQR)	0.712 (0.403, 1.349)	0.431 (0.254, 0.791)	-7.306	<0.01	0.761 (0.441, 1.459)	0.431 (0.258, 0.767)	-8.865	<0.01
aPSADPZ (ng ml <sup>-2</sup> ), median (IQR)	0.213 (0.123, 0.415)	0.074 (0.041, 0.129)	-14.428	<0.01	0.249 (0.142, 0.441)	0.079 (0.044, 0.136)	-11.211	<0.01
PIRADS (n)								
2	2	137	NA	NA	1	138	NA	NA
3	30	171	NA	NA	19	182	NA	NA
4	149	34	NA	NA	122	61	NA	NA
5	176	16	NA	NA	166	26	NA	NA
ISUP (n)								
1	48	NA	NA	NA	NA	NA	NA	NA
2	105	NA	NA	NA	NA	NA	NA	NA
3	94	NA	NA	NA	NA	NA	NA	NA
4	48	NA	NA	NA	NA	NA	NA	NA
5	55	NA	NA	NA	NA	NA	NA	NA

PIRADS: Prostate Imaging Reporting and Data System; PCa: prostate cancer; csPCa: clinically significant prostate cancer; isPCa: clinically insignificant prostate cancer; PSA: prostate-specific antigen; f/tPSA: free/total prostate-specific antigen; PV: prostate volume; PSAD: prostate-specific antigen density; TZV: transitional zone volume; PZV: peripheral zone volume; PSADPZ: prostate-specific antigen density of peripheral zone; aPSADPZ: adjusted prostate-specific antigen density of peripheral zone; ISUP: International Society of Urological Pathology; IQR: interquartile range; PZ-ratio: peripheral zone volume ratio; NA: not available

**Table 2: Univariate regression analyses for various parameters to detect PCa and csPCa**

Characteristic	PCa diagnosis		csPCa diagnosis	
	OR (95% CI)	P	OR (95% CI)	P
Age (year)	1.086 (1.064–1.109)	<0.01	1.086 (1.063–1.108)	<0.01
PSA (ng ml <sup>-1</sup> )	1.053 (1.038–1.069)	<0.01	1.066 (1.049–1.082)	<0.01
f/tPSA	0.001 (0–0.008)	<0.01	0.001 (0–0.002)	<0.01
PV (ml)	0.977 (0.971–0.984)	<0.01	0.979 (0.973–0.986)	<0.01
PSAD (ng ml <sup>-2</sup> )	33.224 (15.152–72.851)	<0.01	46.755 (21.165–103.285)	<0.01
TZV (ml)	0.957 (0.947–0.967)	<0.01	0.959 (0.949–0.970)	<0.01
PZ-ratio	453.766 (139.206–1479.123)	<0.01	335.390 (102.123–1101.477)	<0.01
PSADPZ (ng ml <sup>-2</sup> )	1.865 (1.491–2.332)	<0.01	2.191 (1.736–2.765)	<0.01
aPSADPZ (ng ml <sup>-2</sup> )	1962.141 (416.442–9244.979)	<0.01	2216.515 (498.593–9853.613)	<0.01
PIRADS		<0.01		<0.01
2	Reference		Reference	
3	11.549 (2.708–49.255)		13.574 (1.790–102.915)	
4	261.382 (61.869–1104.267)		256.594 (35.062–1877.828)	
5	662.167 (151.047–2902.831)		808.286 (108.576–6017.217)	

PCa: prostate cancer; csPCa: clinically significant prostate cancer; OR: odds ratio; CI: confidence interval; PSA: prostate-specific antigen; f/tPSA: free/total PSA; PV: prostate volume; PSAD: prostate-specific antigen density; TZV: transitional zone volume; PZ-ratio: peripheral zone volume ratio; PSADPZ: prostate-specific antigen density of peripheral zone; aPSADPZ: adjusted prostate-specific antigen density of peripheral zone; PIRADS: Prostate Imaging Reporting and Data System

other parameters, aPSADPZ showed the highest AUCs of 0.812 and 0.828 for PCa and csPCa diagnosis, followed by PSAD with 0.762 and 0.788, PZ-ratio with 0.748 and 0.735, and PSADPZ with 0.659 and 0.694, respectively (Figure 1). After pairwise comparison, the AUC of aPSADPZ was significantly larger than other parameters for PCa diagnosis (aPSADPZ vs PSA,  $Z$  value: 7.918,  $P < 0.01$ ; aPSADPZ vs PSAD,  $Z$  value: 5.934,  $P < 0.01$ ; aPSADPZ vs PSADPZ,  $Z$  value: 8.802,  $P < 0.01$ ; and aPSADPZ vs PZ-ratio,  $Z$  value: 3.671,  $P < 0.01$ ) and csPCa diagnosis (aPSADPZ vs PSA,  $Z$  value: 6.528,  $P < 0.01$ ; aPSADPZ vs PSAD,  $Z$  value: 5.057,  $P < 0.01$ ; aPSADPZ vs PSADPZ,

$Z$  value: 8.023,  $P < 0.01$ ; and aPSADPZ vs PZ-ratio,  $Z$  value: 5.149,  $P < 0.01$ ).

#### Nomograms and validation of the two models for diagnosing PCa and csPCa

Based on the multivariate regression coefficients, nomograms (Figure 2a and 2b) were used to visualize the predictive results. The calibration and discrimination abilities of these nomograms were further validated with an internal cohort (1000 bootstrap resamples, Figure 2c and 2d) were used. Compared to the base models (including

age, PSA, f/tPSA, and PSAD), the new models exhibited obviously higher AUC values (PCa: 0.945 vs 0.830,  $P < 0.01$ ; and csPCa: 0.937 vs 0.845,  $P < 0.01$ ) for predicting PCa and csPCa (Figure 3a and 3b). Calibration curves showed excellent calibration between the actual and predicted probabilities of the new models for diagnosing PCa and csPCa. The decision curve analysis indicated that the net benefit of new models was better than that of base models for predicting patients with or without PCa (Figure 3c and 3d). In addition, clinical impact curves showed that in high-risk threshold, the number of patients with PCa and csPCa predicted by the new model was in good agreement with the actual number of patients with PCa and csPCa (Figure 3e and 3f).

**DISCUSSION**

The current consensus is that PSA is the most commonly used for PCa screening.<sup>16</sup> Previous research has shown that the PSA cut-off level of 4 ng ml<sup>-1</sup> should be used for the diagnosis of PCa.<sup>17</sup> However, PSA is

found not only in PCa but also in benign prostate hyperplasia (BPH), nonmalignant condition, and inflammatory diseases, which makes it not specific for PCa detection. It is generally believed that BPH occurs mainly because of TZ hyperplasia. Therefore, TZ may increase the level of PSA in BPH patients, while the PSA in the PZ is quite stable. Aminsharifi *et al.*<sup>12</sup> and Kim *et al.*<sup>13</sup> demonstrated that PSAD had better accuracy than PSA in distinguishing between PCa and BPH. Chang *et al.*<sup>14</sup> showed that the PZ-ratio could be used as a predictor of PCa. Koo *et al.*<sup>18</sup> and Lee *et al.*<sup>19</sup> indicated that PZPSAD was better than PSA for the detection of PCa. In this study, we found that PZ-ratio had an advantage over PSA in the diagnosis of PCa, while PSADPZ had no advantage over PSA. PCa is mostly found in the PZ,<sup>20</sup> and tumors in the PZ can increase the levels of PSA in patients with a high PZ-ratio. Our results showed that the aPSADPZ had significant predictive ability in both univariate and multivariate analyses, indicating it was the best predictor of PCa in this study. Compared with PSADPZ, PZ-ratio and PSAD were more important for the diagnosis of PCa. Therefore, PSAD was combined with PZ-ratio to obtain a new index (aPSADPZ), which achieved a better predictive outcome.

Recently, the PIRADS score has shown important clinical significance in PCa diagnosis.<sup>10</sup> In our study, PIRADS also exhibited a significant predictive capability in both univariate and multivariate analyses. Therefore, PIRADS and aPSADPZ were selected to construct a new predictive model. In 1999, Eastham *et al.*<sup>21</sup> reported the first nomogram to predict PCa. However, most of the nomograms only include common variables such as PSA, f/tPSA, PSAD, and others. To our knowledge, this is a new nomogram that combines PIRADS and aPSADPZ. The AUCs of new model from Chang *et al.*<sup>14</sup> (base model + PZ-ratio + PIRADS) for predicting PCa and csPCa were 0.871 and 0.890, respectively. In our study, the AUCs of the new model were 0.945 and 0.937 for PCa and csPCA diagnosis, respectively. Further validation of the new model for diagnosing PCa indicated its excellent

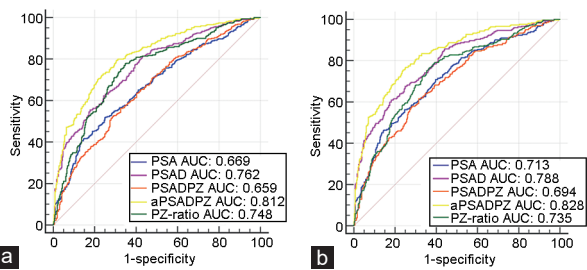


**Figure 1:** ROC curves of various parameters in the diagnosis of (a) PCa and (b) csPCa. PSA: prostate-specific antigen; PSAD: prostate-specific antigen density; PSADPZ: prostate-specific antigen density of peripheral zone; aPSADPZ: adjusted prostate-specific antigen density of peripheral zone; PZ-ratio: peripheral zone volume ratio; PCa: prostate cancer; csPCa: clinically significant prostate cancer; ROC: receiver operating characteristic; AUC: area under curve.

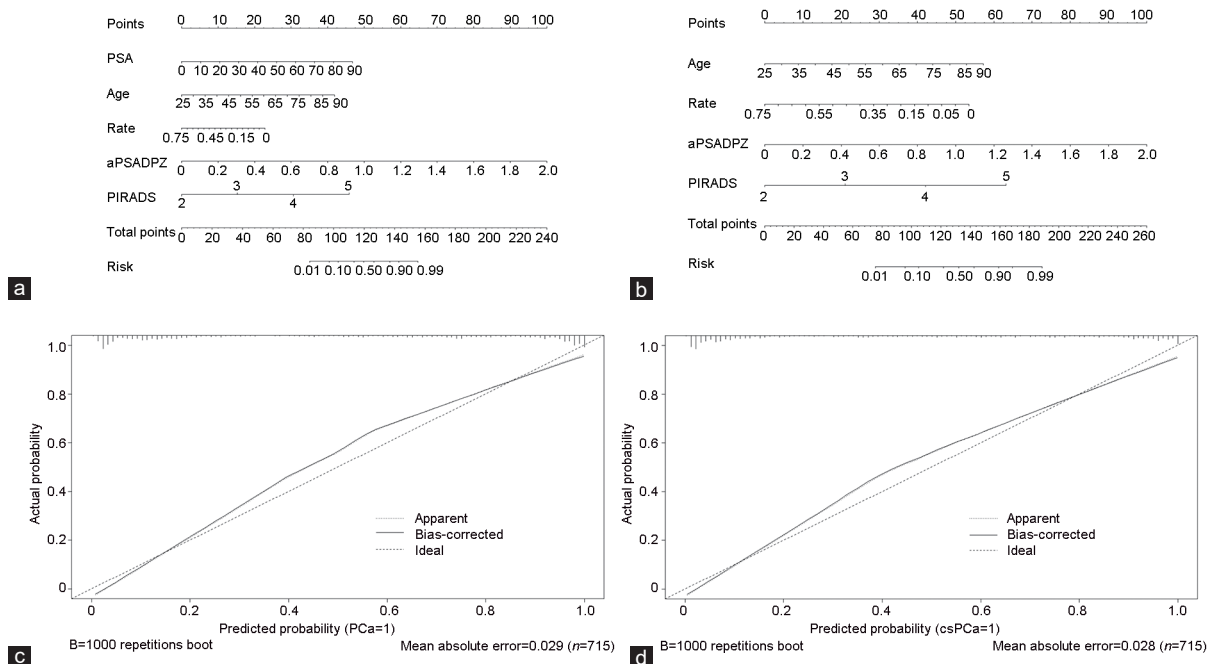


**Figure 2:** Nomogram of two models for predicting the probability of (a) PCa and (b) csPCa. Calibration curves of these two nomograms in the diagnosis of (c) PCa and (d) csPCa. PSA: prostate-specific antigen; aPSADPZ: adjusted prostate-specific antigen density of peripheral zone; PIRADS: Prostate Imaging Reporting and Data System; PCa: prostate cancer; csPCa: clinically significant prostate cancer.

**Table 3: Multivariate regression analysis for various parameters to detect PCa and csPCa**

Characteristic	PCa diagnosis		csPCa diagnosis	
	OR (95% CI)	P	OR (95% CI)	P
Age (year)	1.086 (1.049–1.112)	<0.01	1.071 (1.038–1.106)	<0.01
PSA (ng ml <sup>-1</sup> )	0.945 (0.916–0.975)	<0.01		
f/tPSA	0.033 (0.001–0.723)	0.03	0.005 (0–0.112)	<0.01
aPSADPZ (ng ml <sup>-2</sup> )	636.083 (59.626–6785.640)	<0.01	75.828 (16.502–348.441)	<0.01
PIRADS		<0.01		<0.01
2	Reference		Reference	
3	10.767 (2.469–46.950)		12.14 (1.570–93.875)	
4	166.447 (38.641–716.975)		158.678 (21.395–1176.855)	
5	293.373 (64.792–1328.377)		288.654 (38.067–2188.806)	

PCa: prostate cancer; csPCa: clinically significant prostate cancer; OR: odds ratio; CI: confidence interval; PSA: prostate-specific antigen; f/tPSA: free/total PSA; PV: prostate volume; PSAD: prostate-specific antigen density; aPSADPZ: adjusted prostate-specific antigen density of peripheral zone; PIRADS: Prostate Imaging Reporting and Data System

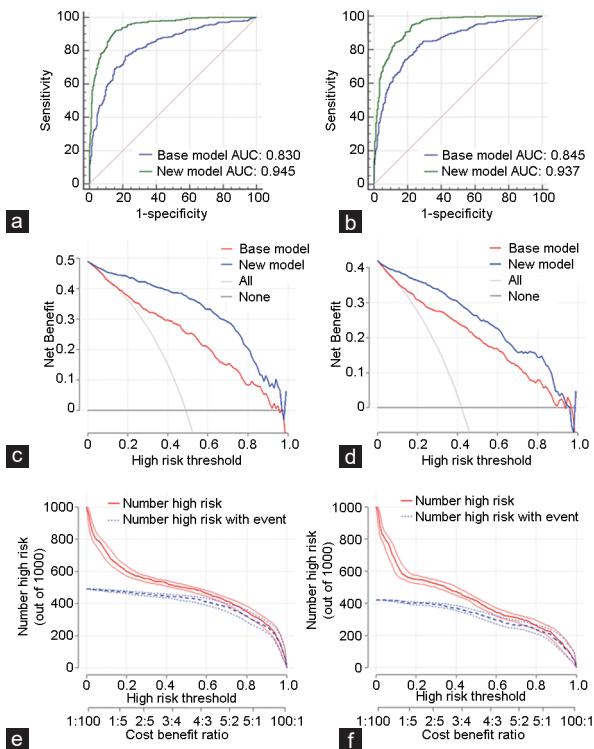


**Figure 3:** ROC curves of the two models in the diagnosis of (a) PCa and (b) csPCa. Decision curve analysis of the two models for predicting the occurrence (c) PCa and (d) csPCa. Clinical impact curves of the two models for the diagnosis of (e) PCa and (f) csPCa. AUC: area under curve; ROC: receiver operating characteristic; PCa: prostate cancer; csPCa: clinically significant prostate cancer.

performance compared with the conventional models consisting of only age, PSA, PV, and PSAD. First, the new model showed significantly higher AUCs than the base model in ROC curves. Second, the net benefit of the new model is higher than that of the base model for nearly all the probability thresholds in the decision curve analysis, which is more suitable for guiding clinical decision-making. Finally, we found a good calibration between the actual and predicted probabilities of the new model. Taken together, aPSADPZ and PIRADS were significant in predicting the occurrence of PCa, which should be combinedly used when building predictive models for PCa diagnosis.

Our study has several limitations. (1) This was a retrospective study performed at a single institution with the possible risk of selection

bias. (2) PIRADS and aPSADPZ required MRI images; therefore, this model cannot be applied to patients who are unable to undergo MRI. (3) PIRADS scores are dependent on the experience of a radiologist, and may vary from physician to physician. (4) The definition of csPCa used in this study does not include all clinically significant diseases because ISUP GG1 with high tumor volume load may be significant and ISUP GG2 with low tumor volume load may be insignificant.

**CONCLUSIONS**

In summary, aPSADPZ has a higher predictive accuracy for the diagnosis of PCa than the conventional indicators, which may decrease the risk of misdiagnosis and reduce the number of unnecessary biopsies. The combination of aPSADPZ with PIRADS can improve PCa detection, increase diagnostic accuracy and avoid unnecessary biopsies.

**AUTHOR CONTRIBUTIONS**

CH helped in project development and data analysis, and wrote the manuscript. FQ was involved in project development and data collection, and wrote the manuscript. ZQC was involved in project development and data analysis and wrote the manuscript. JXP and XMW helped in data analysis. Q LX performed the statistical analysis. XDW helped to draft the manuscript. XJZ, LCG, and JQH helped in data collection. YHH helped in project development and edited the manuscript. All authors have read and approved the final manuscript.

**COMPETING INTERESTS**

All authors declare no competing interests.

**ACKNOWLEDGMENTS**

This work was supported by two grants from the Key Research and Development Program of Jiangsu Province (No. BE2020654 and No. BE2020655) and a grant from the General Program of Jiangsu Health Commission (No. H2019040) and a grant from National Key R&D Program of China (No. 2017YFC0114303). We thank all colleagues for their supports during the data collection and the preparation of this manuscript.

**REFERENCES**

- Siegel RL, Miller KD, Fedewa SA, Ahnen DJ, Meester RG, *et al*. Colorectal cancer statistics, 2017. *CA Cancer J Clin* 2017; 67: 177–93.
- Pang C, Guan Y, Li H, Chen W, Zhu G. Urologic cancer in China. *Jpn J Clin Oncol* 2016; 46: 497–501.
- Taira AV, Merrick GS, Galbreath RW, Andreini H, Taubenslag W, *et al*. Performance of transperineal template-guided mapping biopsy in detecting prostate cancer in the initial and repeat biopsy setting. *Prostate Cancer Prostatic Dis* 2010; 13: 71–7.
- Cooperberg MR, Broering JM, Kantoff PW, Carroll PR. Contemporary trends in low risk prostate cancer: risk assessment and treatment. *J Urol* 2007; 178: S14–9.



- 5 Osses DF, van Asten JJ, Kieft GJ, Tijsterman JD. Prostate cancer detection rates of magnetic resonance imaging-guided prostate biopsy related to Prostate Imaging Reporting and Data System score. *World J Urol* 2017; 35: 207–12.
- 6 Kasivisvanathan V, Rannikko AS, Borghi M, Panebianco V, Mynderse LA, *et al*. MRI-targeted or standard biopsy for prostate-cancer diagnosis. *N Engl J Med* 2018; 378: 1767–77.
- 7 Moore CM, Kasivisvanathan V, Eggener S, Emberton M, Futterer JJ, *et al*. Standards of reporting for MRI-targeted biopsy studies (START) of the prostate: recommendations from an International Working Group. *Eur Urol* 2013; 64: 544–52.
- 8 Rozas GQ, Saad LS, Melo H, Gabrielle HA, Szejnfeld J. Impact of PI-RADS v2 on indication of prostate biopsy. *Int Braz J Urol* 2019; 45: 486–94.
- 9 Polanec S, Helbich TH, Bickel H, Pinker-Domenig K, Georg D, *et al*. Head-to-head comparison of PI-RADS v2 and PI-RADS v1. *Eur J Radiol* 2016; 85: 1125–31.
- 10 Kasel-Seibert M, Lehmann T, Aschenbach R, Guettler FV, Abubrig M, *et al*. Assessment of PI-RADS v2 for the detection of prostate cancer. *Eur J Radiol* 2016; 85: 726–31.
- 11 Muller BG, Kaushal A, Sankineni S, Lita E, Hoang AN, *et al*. Multiparametric magnetic resonance imaging-transrectal ultrasound fusion-assisted biopsy for the diagnosis of local recurrence after radical prostatectomy. *Urol Oncol* 2015; 33: 425.e1–6.
- 12 Aminsharifi A, Howard L, Wu Y, De Hoedt A, Bailey C, *et al*. Prostate specific antigen density as a predictor of clinically significant prostate cancer when the prostate specific antigen is in the diagnostic gray zone: defining the optimum cutoff point stratified by race and body mass index. *J Urol* 2018; 200: 758–66.
- 13 Kim JJ, Suh YS, Kim TH, Jeon SS, Lee HM, *et al*. Establishment and validation of extra-transitional zone prostate specific antigen density (ETzD), a novel structure-based parameter for quantifying the oncological hazard of prostates with enlarged stroma. *Sci Rep* 2019; 9: 770.
- 14 Chang Y, Rui C, Yang Q, Xu G, Sun Y. Peripheral zone volume ratio (PZ-ratio) is relevant with biopsy results and can increase the accuracy of current diagnostic modality. *Oncotarget* 2017; 8: 34836–43.
- 15 Delong ER, Delong DM, Clarke-Pearson DL. Comparing the areas under two or more correlated receiver operating characteristic curves: a nonparametric approach. *Biometrics* 1988; 44: 837.
- 16 Chen CS, Wang SS, Li JR, Cheng CL, Yang CR, *et al*. PSA density as a better predictor of prostate cancer than percent-free PSA in a repeat biopsy. *J Chin Med Assoc* 2011; 74: 552–5.
- 17 Luboldt H, Bex A, Swoboda A, Hüsing J, Rübber H, *et al*. Early detection of prostate cancer in Germany: a study using digital rectal examination and 4.0 ng/ml prostate-specific antigen as cutoff. *Eur Urol* 2001; 39: 131–7.
- 18 Koo KC, Lee DH, Lee SH, Chung BH. Peripheral zone prostate-specific antigen density: an effective parameter for prostate cancer prediction in men receiving 5 $\alpha$ -reductase inhibitors. *Prostate Int* 2013; 1: 102–8.
- 19 Lee J, Yang SW, Jin L, Lee CL, Song KH. Is PSA density of the peripheral zone as a useful predictor for prostate cancer in patients with gray zone PSA levels? *BMC Cancer* 2021; 21: 472.
- 20 Chen ME, Johnston DA, Tang K, Babaian RJ, Troncoso P. Detailed mapping of prostate carcinoma foci: biopsy strategy implications. *Cancer* 2015; 89: 1800–9.
- 21 Eastham JA, May R, Robertson JL, Sartor O, Kattan MW. Development of a nomogram that predicts the probability of a positive prostate biopsy in men with an abnormal digital rectal examination and a prostate-specific antigen between 0 and 4 ng/mL. *Urology* 1999; 54: 709–13.

This is an open access journal, and articles are distributed under the terms of the Creative Commons Attribution-NonCommercial-ShareAlike 4.0 License, which allows others to remix, tweak, and build upon the work non-commercially, as long as appropriate credit is given and the new creations are licensed under the identical terms.

©The Author(s)(2022)

